

High-energy pion-nucleus elastic scattering

C. M. Chen

Los Alamos National Laboratory, Los Alamos, New Mexico 87545

and Department of Physics and Center for Theoretical Physics, Texas A&M University, College Station, Texas 77843

D. J. Ernst

Department of Physics and Center for Theoretical Physics, Texas A&M University, College Station, Texas 77843

and Department of Physics and Astronomy, Vanderbilt University, Nashville, Tennessee 37235

Mikkel B. Johnson

Los Alamos National Laboratory, Los Alamos, New Mexico 87545

(Received 17 December 1992)

We investigate theoretical approaches to pion-nucleus elastic scattering at high energies ($300 \leq T_\pi \leq 1$ GeV). A "model-exact" calculation of the lowest-order microscopic optical model, carried out in momentum space and including the full Fermi averaging integration, a realistic off-shell pion-nucleon scattering amplitude and fully covariant kinematics, is used to calibrate a much simpler theory. The simpler theory utilizes a local optical potential with an eikonal propagator and includes the Coulomb interaction and the first Wallace correction, both of which are found to be important. Comparisons of differential cross sections out to beyond the second minimum are made for light and heavy nuclei. Particularly for nuclei as heavy as ^{40}Ca , the eikonal theory is found to be an excellent approximation to the full theory.

PACS number(s): 25.80.Ek, 24.10.Eq, 24.10.Jv

I. INTRODUCTION

The pion-nucleus interaction on and below the Δ_{33} resonance has been extensively studied, and microscopic models of elastic scattering do a reasonable job [1] of describing the data. The pion-nucleus interaction at energies above the Δ_{33} resonance has received [2-5] much less attention. In this energy region ($300 \text{ MeV} \leq T_\pi \leq 1$ GeV), the pion has a much shorter wavelength. For example, the wavelength at resonance is about 4 fm (about the size of the nucleus), while at 1 GeV the wavelength is 1 fm (about the size of a single nucleon). The shorter wavelength implies that elastic and inelastic data at the higher energies will provide sensitivity to the details of the spatial dependence of the ground-state and transition densities. The data may also prove sensitive to modifications [6, 7] of the properties of the nucleon in the nuclear medium, or reveal significant contributions from exchange currents [8].

Moreover, the pion-nucleon two-body interaction becomes much weaker as one goes to energies above the Δ_{33} resonance. The two-body total cross section becomes less than 30 mb, which is about 15% of that on the Δ_{33} resonance. The first implication of this weaker amplitude is that the pion is able to penetrate deeper into the nucleus. A simple estimate [9] from total reaction cross section studies shows that a projectile can penetrate into a target to a radius that is equal to the impact parameter at which the profile function equals one mean free path. In Fig. 1 the profile functions for ^{12}C , ^{40}Ca , and ^{208}Pb are pictured, and the arrows indicate approximately how far into a nucleus a pion of the labeled energy can penetrate.

The pion in the energy region from 500 MeV to 1 GeV is one of the most penetrating of the strongly interacting particles.

The second implication of the weaker two-body cross section is that multiple-scattering theory for the optical potential becomes increasingly convergent. A simple estimate of the convergence is obtained by comparing a typical second-order term in the optical potential to the first-order term. For the case of short-range correlations, one obtains [10]

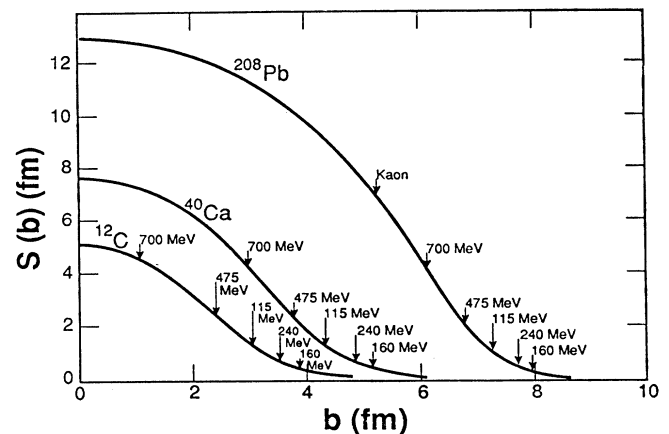


FIG. 1. Profile function $S(b)$ for ^{12}C , ^{40}Ca , and ^{208}Pb . The arrows indicate the depth to which the pion (labeled by its energy) can penetrate.

$$R \equiv \frac{U^{(2)}}{U^{(1)}} = \sqrt{\sigma} \frac{\ell_c}{k} \rho, \quad (1)$$

where σ is the total two-body cross section, ℓ_c is the correlation length, and ρ is the nuclear density at which the pion interacts (see Fig. 1). The factor of $1/k$, where k is the incident pion momentum, reflects the decreasing magnitude of the pion propagator in $U^{(2)}$ with increasing energy. On resonance, we find $R \approx 0.1$, with $R < 1$ only because ρ is so small there. At 500 MeV, we find $R \approx 0.04$ and, at 1 GeV, $R \approx 0.02$. Thus differences between the data and a carefully calculated result utilizing a first-order optical potential would be a strong indication of the presence of unconventional phenomena such as mesonic current contributions, modified nucleon properties in the medium, or other yet to be thought of effects.

One option for calculating high-energy pion scattering is a momentum-space optical-potential approach. This presents the opportunity [11] to calculate the scattering from a lowest-order optical potential including the following features: (1) exact Fermi-averaging integration, (2) fully covariant kinematics [12], normalizations, and phase-space factors, (3) invariant amplitudes [11, 13], and (4) finite-range, physically motivated two-body off-shell [13] amplitudes. Within the multiple-scattering theory developed in Refs. [1, 14] this is an exact calculation of the lowest-order optical potential. A brief review of this approach will be given in Sec. II.

A practical difficulty arises when one wants to use the momentum-space optical model to study high-energy pion-nucleus scattering. As the projectile energy increases, more partial waves are needed in the pion-nucleon two-body amplitudes. Below 300 MeV, only S waves and P waves are needed. Above 300 MeV, D waves become important. F waves become significant above 500 MeV and G waves and H waves above 700 MeV. At the same time the number of pion-nucleus partial waves is increasing at a rate proportional to the pion momentum. At high energies the momentum-space approach becomes prohibitively computer intensive, and one would like to search for a simpler alternative.

The semiclassical theory immediately comes to mind as an alternative to the momentum-space approach. It is often used at high energies not only because it is easier to compute, but also because the simpler character of the theory facilitates obtaining physical insights into the reaction. However, the semiclassical theory is expected to be a good approximation only for local potentials and only when the wavelength is sufficiently short. Because the exact pion-nucleus optical potential appears to be highly nonlocal, we examine the role that nonlocalities play in high-energy pion-nucleus scattering. This is done numerically in momentum space and is presented in Sec. II A. We undertake this study as a first step in obtaining a more quantitative measure of the validity of the semiclassical theory than currently exist in the literature.

In Sec. II B we present our semiclassical model [15]. In order to have a quantitative as well as a simple model for confronting data, we include the Coulomb interaction and the first Wallace correction [16]. We establish the validity of the semiclassical model both by examining the

size of the Wallace correction and by comparing it to the model-exact results obtained in momentum space. Comparisons of the eikonal model to model-exact calculations are made in Sec. III.

A previous similar investigation can be found in Ref. [17]. There a factorized approximation [18] was used in the momentum-space calculations, so that the full nonlocality of the optical potential was not considered. Furthermore, Glauber multiple scattering theory [19] was proposed, whereas we will examine an even simpler model, that of a local optical potential with the scattering solved via an eikonal approximation. A more detailed discussion that compares and contrasts our results with previous work is given in Sec. IV. A summary, conclusions and future prospects are presented in Sec. V.

II. SCATTERING THEORY

At higher energies where the pion-nucleon amplitude becomes a smooth function of energy and is much weaker than on resonance, the first-order optical potential may well be adequate for describing all of the conventional nuclear physics phenomena that enter into the reaction dynamics. Whether this is so remains for further investigation. Independent of this question, there is the question of whether simpler approaches to the calculation of the lowest-order optical potential and the scattering from this potential are reasonably quantitative. It is this question upon which we concentrate here. Below we first review the momentum-space optical potential which serves as our “model-exact” calculation. In momentum space, we examine the importance of the nonlocalities caused by both the resonance propagation and the finite range of the two-body amplitude. Finding that these both can be accurately approximated, we present a simple eikonal model.

Both the optical and the eikonal models use the same target wave functions, which are obtained from Hartree-Fock calculations [20, 21] with spurious center-of-mass motion removed as discussed in Sec. II A. They also use the same on-shell pion-nucleon two-body amplitudes, which are constructed from Arndt’s [22] and Höhler’s [23] phase shifts.

A. Optical potential

A complete description of the momentum-space optical potential that we use can be found in Ref. [11], and a detailed discussion of the covariant kinematics that we use can be found in Ref. [12]. The formal multiple-scattering theory in which this work is embedded is given in Refs. [1, 14]. Here we provide only a brief overview.

The first-order optical potential in the impulse approximation can be written as

$$\begin{aligned} & \langle \mathbf{k}'_{\pi} \mathbf{k}'_A | U_{\text{mo}}(E) | \mathbf{k}_{\pi} \mathbf{k}_A \rangle \\ &= \sum_{\alpha} \int \frac{d^3 k_{A-1}}{2E_{A-1}} \frac{d^3 k'_N}{2E'_N} \frac{d^3 k_N}{2E_N} \langle \Psi'_{\alpha, \mathbf{k}'_A} | \mathbf{k}'_N \mathbf{k}_{A-1} \rangle \\ & \quad \times \langle \mathbf{k}'_{\pi} \mathbf{k}'_N | t(E) | \mathbf{k}_{\pi} \mathbf{k}_N \rangle \langle \mathbf{k}_N \mathbf{k}_{A-1} | \Psi_{\alpha, \mathbf{k}_A} \rangle, \end{aligned} \quad (2)$$

where \mathbf{k}_π , \mathbf{k}_N , and \mathbf{k}_{A-1} are the momenta of the pion, the struck nucleon, and the $A-1$ residual nucleons in the pion-nucleus center-of-momentum frame, respectively. E is the incident energy of the pion and the nucleus (in the pion-nucleus center-of-momentum frame also), and α is a set of quantum numbers that specifically label the nuclear bound state.

The target wave function $\langle \mathbf{k}_N \mathbf{k}_{A-1} | \Psi_{\alpha, \mathbf{k}_A} \rangle$ defined covariantly [11] contains a momentum-conserving delta function $\delta(\mathbf{k}_A - \mathbf{k}_N - \mathbf{k}_{A-1})$ and is a function of the relative momentum between the nucleon and the $A-1$ residual nucleons. The pion-nucleon t matrix similarly contains a momentum-conserving delta function and is a function of the relative momentum between the pion and the nucleon, $\boldsymbol{\kappa}$,

$$\begin{aligned} & \langle \mathbf{k}'_N \mathbf{k}'_\pi | t(E) | \mathbf{k}_N \mathbf{k}_\pi \rangle \\ &= \delta(\mathbf{k}'_N + \mathbf{k}'_\pi - \mathbf{k}_N - \mathbf{k}_\pi) \langle \boldsymbol{\kappa}' | t[\omega_\alpha(E, \mathbf{k}_\pi, \mathbf{k}_N)] | \boldsymbol{\kappa} \rangle. \end{aligned} \quad (3)$$

One of these three momentum-conserving delta functions leads to overall momentum conservation; the others allow one to perform two of the three integrals in Eq. (2). The remaining integral is the Fermi-averaging integration which must be performed numerically. The details of how we perform the integration can be found in [11].

The energy at which one evaluates the two-body t matrix, $\omega_\alpha(E, \mathbf{k}_\pi, \mathbf{k}_N)$, must be carefully chosen [24] if a convergent perturbation theory is to result for calculations at and below the Δ_{33} resonance region. The energy ω_α is defined covariantly by first defining the energy available to the pion-nucleon two-body subsystem,

$$E_{\pi N} = E - \sqrt{(\mathbf{k}_\pi + \mathbf{k}_N)^2 + m_{A-1}^2}, \quad (4)$$

and then defining the invariant center-of-momentum energy for this system,

$$\omega_\alpha^2 = E_{\pi N}^2 - (\mathbf{k}_\pi + \mathbf{k}_N)^2. \quad (5)$$

The mass of the $A-1$ system, m_{A-1} , differs from the mass of the A -body target, m_A , by a nucleon mass and a binding energy, $m_A = m_{A-1} + m_N + E_b$. This energy must then be shifted by a ‘‘mean-spectral energy’’ E_{MS} , which is a calculated number [24] that approximately accounts for the interaction of the intermediate Δ_{33} (or the intermediate nucleon or other hadronic resonance) with the residual nucleus. This first-order potential produces results for energies near the Δ_{33} resonance that are in remarkable agreement with the data. This is because [1] the sums of the second-order effects (Pauli exclusion, true absorption, and correlation corrections) cancel among themselves. The use of invariant normalizations, invariant phase space, and invariant amplitudes produces the phase-space factors that are present in Eq. (2).

The optical potential so defined is then inserted into the Klein-Gordon equation (with a linear potential) which is solved numerically to produce our model-exact calculation.

B. Eikonal model

The eikonal model we propose to examine results from first replacing the optical potential of Eq. (2) by a local potential and then solving for the scattering amplitude arising from the use of the local potential and the eikonal propagator. In order to include the Coulomb interaction, we divide the scattering amplitude as

$$F(q) = F_{pt}(q) + F_{CN}(q), \quad (6)$$

where q is the momentum transferred to the pion, $\mathbf{q} = \mathbf{k}'_\pi - \mathbf{k}_\pi$, F_{pt} is the point Coulomb scattering amplitude, and F_{CN} is the scattering amplitude calculated from the sum of the strong nuclear potential plus a Coulomb correction, which is the difference between the point Coulomb interaction and the Coulomb interaction of a finite charge distribution. The eikonal approximation gives for $F_{CN}(q)$

$$F_{CN}(q) = ik_\pi \int_0^\infty b db J_0(qb) e^{i\chi_{pt}(b)} \Gamma_{CN}(E, b), \quad (7)$$

where k_π is the momentum of the incident pion in the pion-nucleus center-of-momentum frame, b is the impact parameter, χ_{pt} is the point Coulomb phase (in the eikonal approximation), and Γ_{CN} is the profile function defined below.

In order to incorporate the distortion and energy shift caused by the Coulomb interaction, we follow the prescription given in Ref. [25] and write the profile function as

$$\begin{aligned} \Gamma_{CN}(E, b) &= 1 - \exp\{i\chi_{CN}(E, b)\} \\ &= 1 - \exp\{i\chi_N[E, b(1 + EV_C(b)/k_\pi^2)] \\ &\quad + i\chi_C(b) - i\chi_{pt}(b)\}, \end{aligned} \quad (8)$$

where V_C is the Coulomb potential of a uniformly charged sphere, χ_C is the phase shift caused by that potential, and the nuclear phase shift χ_N is written as

$$\chi_N(E, b) = -\frac{1}{2k_\pi} \int_{-\infty}^\infty dz U_{\text{eik}}[E - V_C(r), r], \quad (9)$$

where

$$r = (b^2 + z^2)^{1/2}, \quad (10)$$

and U_{eik} is the strong potential obtained as follows. First we construct a local potential U_0 from the pion-nucleon two-body scattering amplitude and the target density by

$$\begin{aligned} U_0(E, r) &= -4\pi Z \left[f_p(0)\rho_p + \frac{f'_p(0)}{2k_\pi^2} \nabla^2 \rho_p \right] \\ &\quad - 4\pi N \left[f_n(0)\rho_n + \frac{f'_n(0)}{2k_\pi^2} \nabla^2 \rho_n \right], \end{aligned} \quad (11)$$

where Z and N are the proton number, and the neutron number, respectively. The scattering amplitude $f_p(0)$ [$f_n(0)$] is the pion-proton [pion-neutron] scattering amplitude in the forward direction in the pion-nucleus center-of-momentum frame. The finite range of the pion-nucleon interaction is included through lowest nonvanish-

ing order and produces the additional terms in Eq. (11) which are proportional to the derivatives of the scattering amplitude as shown in Appendix B.

In order to investigate the importance of the lowest-order corrections to the eikonal propagator as derived by Wallace [16], we next replace the potential $U_0(E, r)$ by the potential

$$U_{\text{eik}}(E, r) = U_0 + \frac{U_0^2}{4k_\pi^2} \left(1 + \frac{2b^2}{r} \frac{d}{dr} \ln U_0 \right). \quad (12)$$

This correction (and higher orders) were derived by Wallace [16] as a double expansion of the Fourier-Bessel representation of the t matrix. The corrections can be interpreted as correcting for the straight-line path and for the change in energy along the path. The size of the corrections are estimated in [16], but a quantitative understanding is best found by explicit calculation.

III. RESULTS

In this section we investigate the importance of some of the ingredients of our model-exact calculation of high-energy pion-nucleus scattering. We will then examine how well our simple eikonal theory reproduces the results of the model-exact theory.

A. Contributions from nonlocalities in the optical potential

The most difficult part of evaluating the optical potential in the model-exact theory is performing the Fermi-averaging integration. This is known to be very important in the region of the Δ_{33} resonance, where proper accounting for the recoil and propagation of the pion-nucleus resonance requires a careful treatment of the dependence of the energy ω_α in Eq. (5) on the momentum of the nucleon. Resonance propagation manifests itself as a nonlocality in the optical potential, and this represents the first source of nonlocality whose importance we want to assess for high-energy pions.

To investigate this we calculate elastic scattering of π^- from ^{40}Ca first with full Fermi averaging and then utilizing a closure approximation. The closure approximation that we use results from taking

$$\omega_\alpha^2 = W_{\pi N}^2 - k_\pi^2 \quad \text{and} \quad W_{\pi N} = E - \sqrt{k_\pi^2 + m_{A-1}^2}. \quad (13)$$

This is equivalent to setting the momentum of the struck nucleon to zero in the pion-nucleus c.m. frame.

On the delta resonance, it has been found [26–28] that the closure approximation is totally inadequate and even the “optimally factorized” approximation [28] is not quantitative. At these higher energies the conclusion is not *a priori* clear. The pion-nucleon amplitude is, partial wave by partial wave, rather energy dependent as the individual partial waves are resonant. The total amplitude, however, exhibits only two very broad smooth peaks on a large background.

The resulting differential cross sections for pions at 500 MeV scattering from ^{40}Ca are shown in Fig. 2. We see that the correct treatment of the recoil of the two-body pion-nucleon system only affects the depth of the minimum but not to a very significant degree.

The behavior of the pion-nucleon scattering amplitude off shell is taken from the doorway-resonance model of Ref. [13]. Amplitudes which are resonant are separable in their dependence on the relative momenta, hence maximally nonlocal. This is the second source of nonlocality whose importance we want to investigate. In the doorway-resonance model, in each angular momentum, spin, and isospin channel,

$$\langle \kappa' | t_{JLI}(\omega_\alpha) | \kappa \rangle = \frac{v(\kappa')}{v(\kappa_0)} \langle \kappa_0 | t_{JLI}(\omega_\alpha) | \kappa_0 \rangle \frac{v(\kappa)}{v(\kappa_0)}, \quad (14)$$

where κ_0 is the on-shell momentum, i.e., the momentum corresponding to the center-of-momentum energy ω_α . This nonlocality, which is also factored in the delta-hole [26] model, was found quite important [28] for energies on and below the Δ_{33} resonance. For numerical convenience, we take the form factor to be a Gaussian, $v(\kappa) = \exp(-\kappa^2/\beta^2)$, and we vary β from 500 MeV to 4 GeV to investigate the importance of this nonlocality.

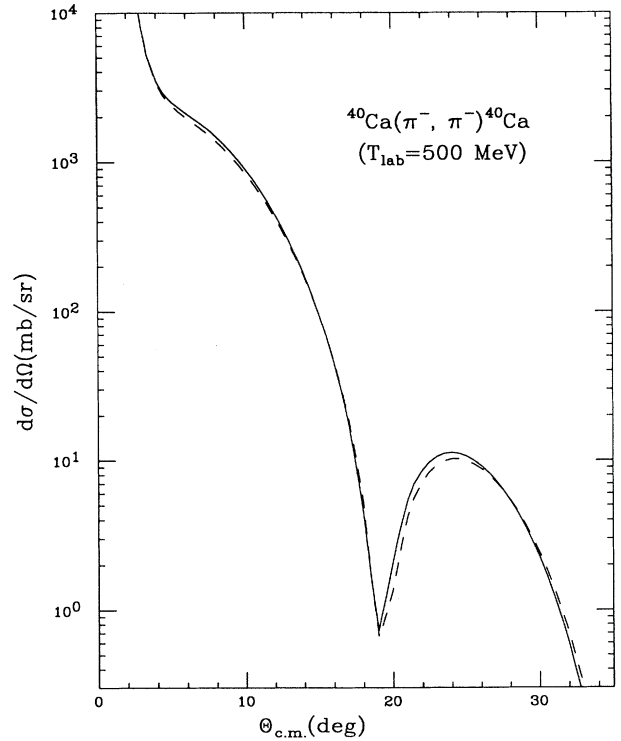


FIG. 2. Differential cross section for elastic scattering of π^- from ^{40}Ca at 500 MeV versus center-of-mass angle. The solid curve is the result of a calculation in which the full Fermi averaging is performed exactly, while the dashed curve uses the closure approximation defined in Eq. (13).

The differential cross sections for π^- - ^{40}Ca scattering calculated with this variation in the form-factor range are shown in Fig. 3. We see that the dependence on the off-shell range is weak at this energy.

There exists some confusion in the literature concerning the possible values for β . First, if one does not include invariant phase-space factors explicitly, they will appear effectively in what one might wish to call the form factor. This difference is then one of semantics. However, in deciding what might be a reasonable range over which to vary the form factor, one should treat the kinematic factors explicitly. In the P -wave channels, an artificial and incorrect increase (in coordinate space) in the range of the form factor will also result if the pion-nucleon pole term [29] is not included in the model of the pion-nucleon amplitude. For our purposes here, the difference of interest is in examining how the cross section changes in going from the physically motivated doorway-model form factors to the higher momentum cutoff. The 4 GeV cutoff produces an approximately zero-range interaction in coordinate space. Figure 3 demonstrates that the nonlocalities contained in a finite-range interaction do not alter significantly the predicted elastic cross sections for these high-energy pions.

We have found that the nonlocalities in the optical potential at high energies do not have an important effect. This suggests that the simple eikonal approach outlined

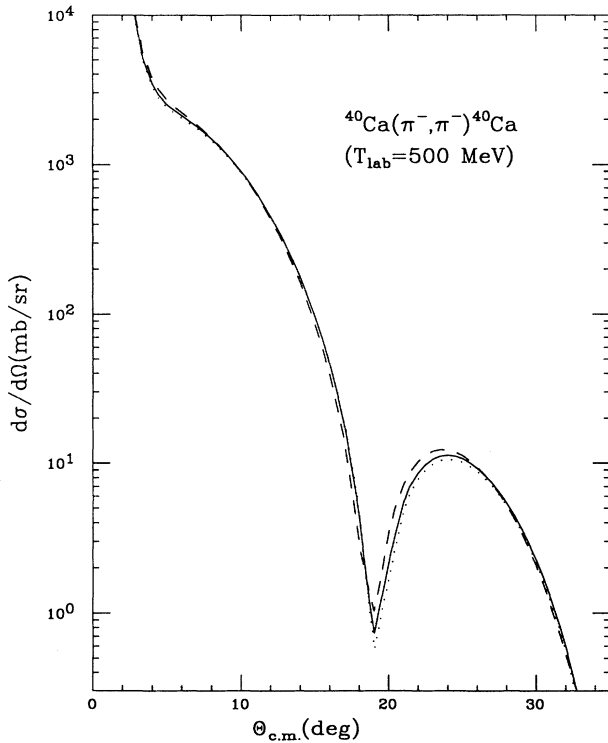


FIG. 3. Differential cross section calculated from different form factor ranges β defined in Sec. III for π^- - ^{40}Ca elastic scattering at 500 MeV. The solid curve is from the "model-exact" theory. The dotted curve corresponds to $\beta = 4$ GeV. The dashed curve is the result from setting $\beta = 500$ MeV.

above could prove to be an adequate model for quantitative work at these energies. To investigate this, we picture the differential cross sections predicted by each model for π^\pm - ^{12}C and π^\pm - ^{40}Ca at 800 MeV/c in Fig. 4 and Fig. 5. The data are from Ref. [4]. As stated earlier, we construct the target density from the same wave functions as were used in the momentum-space calculation and use the same on-shell pion-nucleon scattering amplitude. For ^{40}Ca , both the location of the minima and the magnitude of the cross section at the forward angles are in good agreement. The agreement is, however, not as quantitative for ^{12}C where the minima are slightly shifted. This difference is presumably caused in part by the fact that the kinematics of target recoil enter explicitly in the momentum-space formulation but not in the eikonal approach. The eikonal model is thus more quantitative for the heavier nuclei. We are examining the eikonal model to see if it can be further improved for the light nuclei.

The data from Ref. [4] have a quoted accuracy for the overall normalization of 15%. The discrepancy we find is larger than this. Before concluding that the difference demands an enhanced, in the medium, pion-nucleon amplitude, we feel it is prudent to wait for data presently being taken (at 400 and 500 MeV at LAMPF, from 300 MeV to 1 GeV at KEK, and at similar energies at the AGS at Brookhaven) before reaching a definitive conclusion.

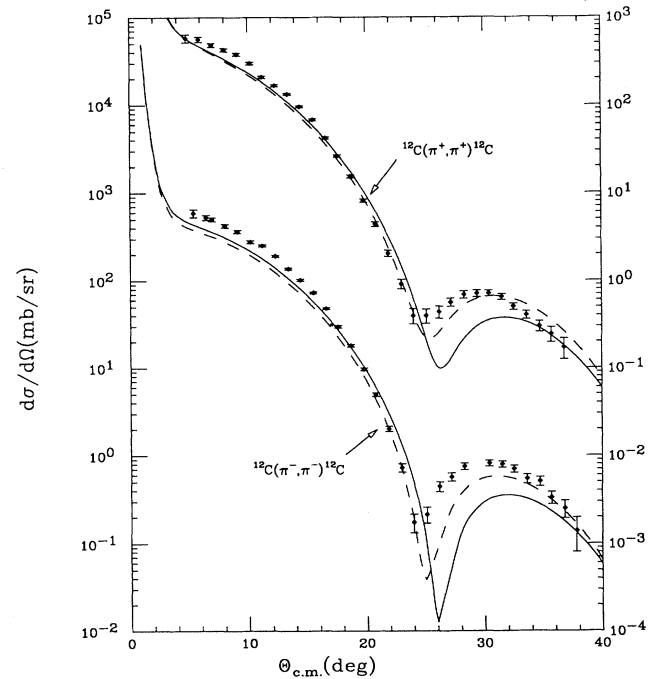


FIG. 4. Elastic differential cross sections for π^\pm - ^{12}C scattering at a pion laboratory momentum 800 MeV/c. The solid curves are from the momentum-space calculations, while the dashed curves are from the eikonal model. Data are obtained from Ref. [4].

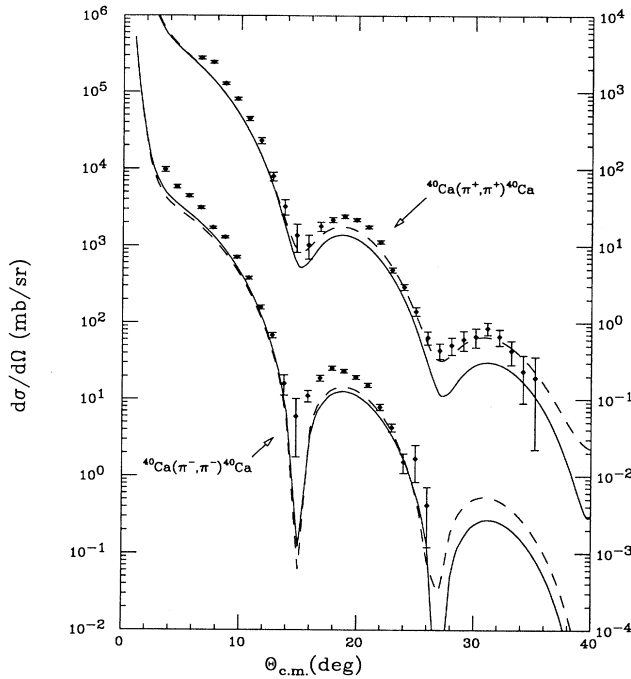


FIG. 5. Same as Fig. 4 except the target is ^{40}Ca .

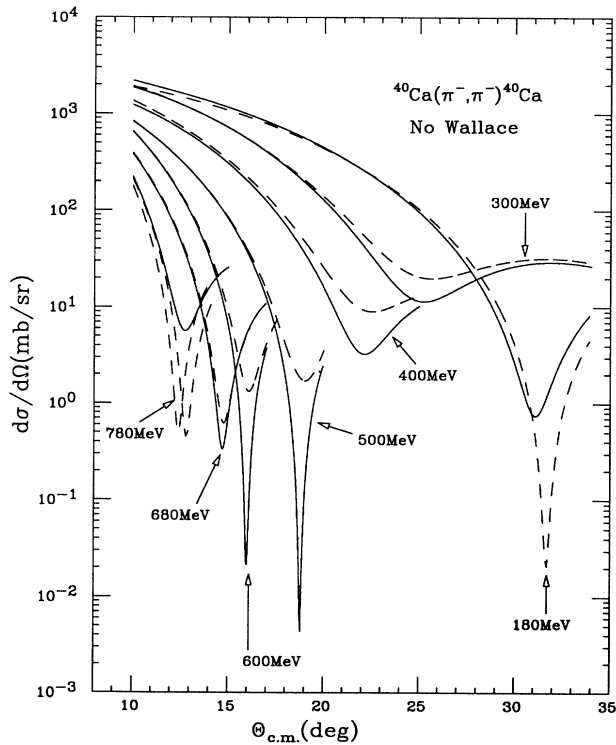


FIG. 6. π^- - ^{40}Ca elastic differential cross section calculated from the eikonal model at labeled pion laboratory energies. The Coulomb interaction is included in all the solid curves, but not the dashed curves. The Wallace correction is not included here.

B. Important features in the eikonal approximation

In this section we investigate the role of the Coulomb interaction and the first Wallace correction, which are both necessary if one wants to use the eikonal model to quantitatively approximate the results of the solution of the model-exact theory.

First, we find that the Coulomb interaction plays an important role in determining the depth of the minima in the differential cross section. To see exactly how important Coulomb-nuclear interference is, we compare the calculation of the π^- - ^{40}Ca differential cross section at a series of energies as shown in Fig. 6 with and without the Coulomb interaction. The Wallace correction is not included in either the solid or the dashed curves. We find that the first minimum in the differential cross sections becomes very deep when the Coulomb interaction is included, falling well below 10^{-2} mb/sr in the region of 500–600 MeV. Without the Coulomb interaction, the deepest minimum is much shallower and occurs at 780 MeV. The inclusion of the Coulomb interaction in the theory is necessary if a quantitative comparison with the data for π^- - ^{40}Ca is to be made. Coulomb-nuclear interference is destructive for π^- and constructive for π^+ , which produces a less dramatic effect for π^+ - ^{40}Ca scattering in this energy region.

Wallace has shown in Ref. [16] that the semiclassical

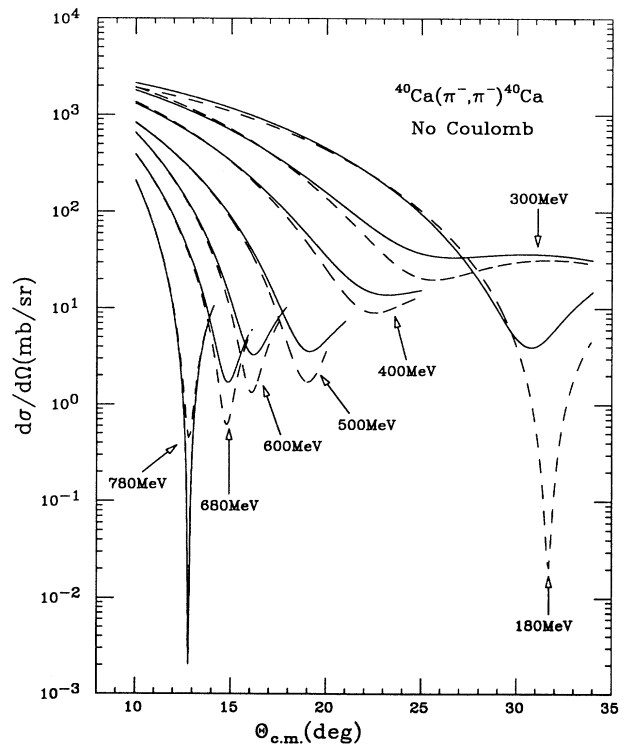


FIG. 7. π^- - ^{40}Ca elastic differential cross sections calculated from the eikonal model at labeled pion laboratory energies. The dashed curves are the same as in Fig. 6. The solid curves include the Wallace correction, but not the Coulomb interaction.

approximation can be improved if higher-order corrections (known as “Wallace” corrections) are included. We examine in Fig. 7 the importance of the first Wallace correction, Eq. (12), for π^- - ^{40}Ca scattering. We see in Fig. 7, in the absence of the Coulomb interaction, that the Wallace correction is dramatic on resonance, $T_\pi = 180$ MeV, where it fills in the deep minimum. At higher energies, the correction interferes constructively until about 700 MeV filling in the minima somewhat. At 780 MeV, however, the Wallace correction interferes destructively with U_0 and produce a much deeper minimum.

In Fig. 8 we turn on both the Coulomb interaction and the Wallace correction; we find a fascinating interplay between the two. Note that at 400 MeV, for example, the two corrections are out of phase and tend to cancel. At 680 MeV, however, they are in phase and interfere destructively with U_0 , producing the very deep minimum. By 780 MeV they are both out of phase with each other but in phase with the lowest-order term and thus fill in the minima. Both the Coulomb and the Wallace corrections are necessary if there is to be a deep minima at 680 MeV, and not at the neighboring energies. We note that the data of Ref. [4] were taken at a pion laboratory momentum of 800 MeV/c, which is very near $T_\pi = 680$ MeV. The depth of the first minimum of the differential cross section for π^- scattering over the energy range 400–800 MeV should prove a very sensitive test of the

existence, or lack thereof, of higher-order corrections in the reaction dynamics.

IV. COMPARISON TO OTHER WORK

Other work on high-energy pion-nucleus elastic scattering, which utilizes the full Glauber theory, can be found in Refs. [17, 30]. In particular, a comparison between the Glauber theory and the optical model on π^\pm - ^{12}C has been made in Ref. [17] and the two approaches were found to be in good agreement at higher energies. We earlier noted that the optical-potential model there did not include the full Fermi averaging, and it was not clear to what extent the agreement found was caused by the approximate treatment of the nonlocalities in the optical potential. Our work clarifies that. We also note that the Glauber theory they used is considerably more complicated than our eikonal model. To our knowledge, the Wallace corrections have not been included in any of the numerical tests of the eikonal model in this energy region. Hence, the important interplay between the Wallace and Coulomb corrections that we find has not been previously noted. We also found that the center-of-mass corrections in the target wave functions are important for ^{12}C but not for ^{40}Ca , which is in agreement with Ref. [17]. Our work strongly supports their conclusion that pion scattering at higher energies becomes theoretically and computationally simpler to treat at a quantitative level.

V. SUMMARY, CONCLUSIONS, AND FUTURE PROSPECTS

We have compared the scattering from the fully microscopic and nonlocal lowest-order optical potential to the scattering from a simple local potential in the eikonal approximation. We have investigated the importance of several features of the full model. Within the framework of our “model-exact” optical model, these include Fermi averaging and the off-shell behavior of the pion-nucleon scattering amplitude. For the eikonal theory, we examine the importance of the first Wallace correction and find that this correction is responsible for a noticeable improvement of the eikonal theory in comparison to the “model-exact” theory. In all cases, the Coulomb-nuclear interference is important and must be included if one is to compare with data.

This semiclassical eikonal theory put forth here is very simple, even simpler than the Glauber theory utilized by others. It appears to be quantitatively valid at high energy, at least for the first several minima in the differential elastic cross section. This makes possible a much simpler reaction theory than has been needed at energies at and below the Δ_{33} resonance.

We have here only examined elastic scattering. We plan to extend this work to inelastic scattering in a distorted wave impulse approximation. At that point we would also be able to address the question of how well the eikonal approach can reproduce not only the elastic cross sections, but how well it can reproduce the distorted wave functions as well.

At high energies and/or for heavy nuclei, use of the full

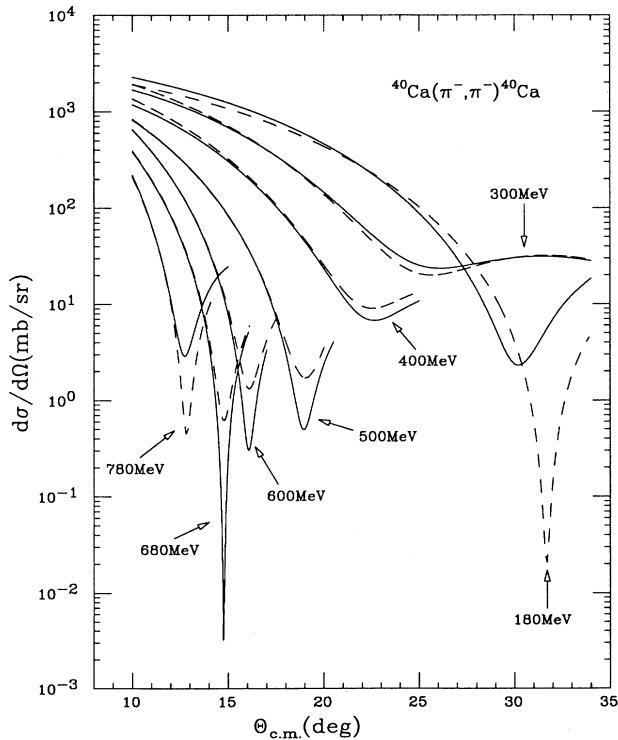


FIG. 8. Dashed curves are the same as in Figs. 6 and 7. The solid curves now contain both the Wallace correction and the Coulomb interaction.

momentum-space optical model becomes very time consuming and sometimes computationally impossible. In contrast, the eikonal theory is relatively simple and fast on the computer. It therefore becomes a matter of considerable practical importance to realize that the physics is faithfully reproduced by the simple version of the theory out to the position of the second minimum in the differential cross section.

An examination of the pion-nucleon cross section shows the complex interplay of resonances. Ultimately, it is interesting to explore how resonances behave in the nucleus and how the specific features of the optical potential are suited for nuclear structure studies. In this pursuit, it will be very helpful to have a simple version of the theory as developed here. We will pursue these questions in subsequent work.

The momentum-space optical model has been extended to treat kaon-nucleus scattering [32]. Results show qualitative agreement with previous work [6]. Modifications to the kaon-nucleon amplitudes in the nuclear medium are needed to eliminate discrepancies between the theory and the data. On the quantitative level, results from the momentum-space approach give larger discrepancies between theory and data than do those from the coordinate-space calculations used in Ref. [6]. Our eikonal model, which is also a coordinate-space approach and been shown to be a good approximation to the “model-exact” momentum-space theory for high-energy pion scattering, can also be modified to treat the kaon scattering. Results from the eikonal model may reveal the sources of the discrepancies between the momentum-space and the previous coordinate-space calculations. Work on the kaon-nucleus scattering utilizing the eikonal model is in progress.

APPENDIX A: CENTER-OF-MASS CORRECTIONS

The scattering theory developed in Ref. [11] is covariant. However, to implement it covariantly would require a covariant model of the nucleus. This would clearly be overkill as the nucleus for the cases of interest is not moving relativistically. A Galilean invariant model would thus suffice. Contemporary models of the nucleus, however, are not Galilean invariant. We use Hartree-Fock models of the nucleus which contain spurious center-of-mass motion. The approach we adopt is discussed in detail in Ref. [12]. The Hartree-Fock results are fitted to elastic electron scattering. The spurious center-of-mass motion is there treated by requiring that momentum conservation holds for average values. We make the same approximation for pion-nucleus scattering.

Specifically we calculate the target wave functions from the Hartree-Fock model and then calculate the Fourier transform of the density. We require the intrinsic density, i.e., the density without the center-of-mass motion. If the wave function were a pure harmonic oscillator, then the correction could be made exactly. Here, we make the correction as if the Hartree-Fock result were exactly a harmonic oscillator. The result [31] for obtaining the in-

trinsic proton density $\rho_{\text{c.m.}}^p$ from the Hartree-Fock density ρ_{HF}^p is

$$\rho_{\text{c.m.}}^p(r) = \int d^3r_1 (B\sqrt{\pi})^{-3} e^{(r_1^2/B^2)} \rho_{\text{HF}}^p(|\mathbf{r} - \mathbf{r}_1|), \quad (\text{A1})$$

where $B = b/\sqrt{A}$ and b is the usual harmonic oscillator parameter. The Hartree-Fock calculation uses a slightly different b for each orbital, and so we use the average value in making the center-of-mass correction.

We use $\rho_{\text{c.m.}}^p$ to calculate the rms radius and compare this to the rms radius measured in electron scattering (with the finite size of the proton removed). For ^{12}C and the Hartree-Fock result from Ref. [21], we find that the rms radius is 2.365 fm from the Hartree-Fock calculation while it is measured to be 2.297 fm in electron scattering. We therefore scale the b 's in the Hartree-Fock calculation by 0.9715 (a 3% correction) so that the correct measured rms radius is reproduced. After the scaling, we calculate the predicted electron scattering and find that these wave functions reproduce electron scattering data out to a momentum transfer which is larger than is encountered in pion scattering. For ^{40}Ca , these corrections were already made by Negele [20] and his wave functions are consistent with the electron scattering data.

APPENDIX B: FORWARD SCATTERING AMPLITUDE

Using a Taylor expansion, we can write the forward scattering amplitude for small angles as

$$\begin{aligned} f(\theta) &\approx f(0) + \left. \frac{df(\theta)}{d\cos\theta} \right|_{\cos\theta=1} (\cos\theta - 1) \\ &\approx f(0) - f'(0) \frac{\theta^2}{2}, \end{aligned} \quad (\text{B1})$$

where

$$\begin{aligned} f'(0) &= \left. \frac{df(\theta)}{d\cos\theta} \right|_{\cos\theta=1} \\ &= \sum_l f_l(0) \left. \frac{dP_l(\cos\theta)}{d\cos\theta} \right|_{\cos\theta=1} \\ &= \sum_l f_l(0) \frac{l(l+1)}{2}. \end{aligned} \quad (\text{B2})$$

We further use the approximation

$$\theta \approx \frac{q}{k_\pi}, \quad (\text{B3})$$

and the fact that the momentum transfer q in momentum space corresponds to $i\nabla$ in coordinate space, to rewrite Eq. (B1) as

$$f(\theta) \approx f(0) + \frac{f'(0)}{2k_\pi^2} \nabla^2. \quad (\text{B4})$$

To construct a local optical potential, we multiply $f(\theta)$ by the target density ρ and obtain Eq. (11).

The forward scattering amplitude $f(0)$ and its derivative $f'(0)$ are calculated from phase shifts in the pion-nucleon c.m. frame and then transferred to the pion-nucleus c.m. frame through the relation

$$f(0) = \frac{k_\pi}{\kappa} f_{\pi N}(0), \quad (\text{B5})$$

where κ and $f_{\pi N}(0)$ denote the pion momentum and forward scattering amplitude in the pion-nucleon c.m. frame.

-
- [1] M. B. Johnson and D. J. Ernst, *Ann. Phys. (N.Y.)* **219**, 266 (1992); C. M. Chen, D. J. Ernst, and M. B. Johnson, *Phys. Rev. C* **47**, R9 (1993).
- [2] S. H. Rokni *et al.*, *Phys. Lett. B* **202**, 35 (1988); G. E. Parnell, D. J. Ernst, and D. R. Giebink, *ibid.* **205**, 135 (1988).
- [3] A. L. Williams *et al.*, *Phys. Lett. B* **216**, 11 (1989).
- [4] D. Marlow, P. D. Barnes, N. J. Colella, S. A. Dytman, R. A. Eisenstein, R. Grace, P. Pile, F. Takeutchi, W. R. Wharton, S. Bart, D. Hancock, R. Hackenberg, E. Hungerford, W. Mayes, L. Pinsky, T. Williams, R. Chrien, H. Palevsky, and R. Sutter, *Phys. Rev. C* **30**, 1662 (1984).
- [5] *The User's View for the Future of LAMPF, 1989; Reports from the Pion Physics Working Group*, edited by G. R. Burleson and D. J. Ernst (Los Alamos National Laboratory Report LA-11673-MS); D. Dehnhard and D. J. Ernst, in *PILAC Users Group Report on Physics with PILAC* (Los Alamos Report LA-UR-92-150).
- [6] P. B. Siegel, W. B. Kaufmann, and W. R. Gibbs, *Phys. Rev. C* **30**, 1256 (1984); **31**, 2184 (1985).
- [7] G. E. Brown, C. B. Dover, P. B. Siegel, and W. Weise, *Phys. Rev. Lett.* **26**, 2723 (1988).
- [8] M. F. Jiang and D. S. Koltun, *Phys. Rev. C* **46**, 2462 (1992).
- [9] D. J. Ernst, *Phys. Rev. C* **19**, 896 (1979).
- [10] D. J. Ernst, J. T. Londergan, G. A. Miller, and R. M. Thaler, *Phys. Rev. C* **16**, 537 (1977).
- [11] D. R. Giebink and D. J. Ernst, *Comput. Phys. Commun.* **48**, 407 (1988).
- [12] D. J. Ernst and G. A. Miller, *Phys. Rev. C* **21**, 1472 (1980); D. L. Weiss and D. J. Ernst, *ibid.* **26**, 605 (1982); D. R. Giebink, *ibid.* **25**, 2133 (1982).
- [13] D. J. Ernst, G. E. Parnell, and C. Assad, *Nucl. Phys.* **A518**, 658 (1990).
- [14] M. B. Johnson and D. J. Ernst, *Phys. Rev. C* **27**, 709 (1983).
- [15] J. Germond and M. B. Johnson, *Phys. Rev. C* **22**, 1622 (1980); J. Germond, M. B. Johnson, and J. A. Johnstone, *ibid.* **32**, 983 (1985).
- [16] S. J. Wallace, *Ann. Phys. (N.Y.)* **78**, 190 (1973); *Phys. Rev. D* **8**, 1846 (1973); *Phys. Rev. C* **8**, 2043 (1973).
- [17] M. Arima, K. Masutani, and R. Seki, *Phys. Rev. C* **44**, 415 (1991).
- [18] K. A. Eisenstein and F. Tabakin, *Comput. Phys. Commun.* **12**, 237 (1976).
- [19] T. Glauber, *Lectures in Theoretical Physics* (Interscience, New York, 1959), Vol. I, p. 315.
- [20] J. W. Negele, *Phys. Rev. C* **1**, 1260 (1969).
- [21] M. Beiner, H. Flocard, N. Van Gai, and P. Quentin, *Nucl. Phys.* **A238**, 29 (1975).
- [22] R. Arndt, computer code SAID, *Phys. Rev. D* **28**, 97 (1983).
- [23] G. Höhler, in *PN Newsletter No. 1*, edited by G. Höhler and B. M. K. Nefkins (Karlsruhe, 1984); R. Koch, *Z. Phys. C* **29**, 597 (1985).
- [24] D. J. Ernst and M. B. Johnson, *Phys. Rev. C* **32**, 940 (1985); D. J. Ernst, D. R. Giebink, and M. B. Johnson, *Phys. Lett. B* **182**, 242 (1986).
- [25] J. Germond and C. Wilkin, *Ann. Phys. (N.Y.)* **121**, 285 (1979).
- [26] M. Hirata, J.-H. Koch, F. Lenz, and E. J. Moniz, *Ann. Phys. (N.Y.)* **120**, 205 (1979).
- [27] L. C. Liu and C. M. Shakin, *Prog. Part. Nucl. Phys.* **5**, 207 (1982).
- [28] D. J. Ernst, G. A. Miller, and D. L. Weiss, *Phys. Rev. C* **27**, 2733 (1983).
- [29] D. J. Ernst and M. B. Johnson, *Phys. Rev. C* **17**, 247 (1978).
- [30] E. Oset and D. Strottman, *Phys. Rev. C* **44**, 468 (1991).
- [31] J. P. Elliot and T. H. R. Skyrme, *Proc. Soc. London A* **232**, 561 (1955).
- [32] C. M. Chen and D. J. Ernst, *Phys. Rev. C* **45**, 2011 (1992).